MOLECULAR PHARMACOLOGY, 18, 384–394

Anatoxin-a: A Novel, Potent Agonist at the Nicotinic Receptor

C. E. SPIVAK,* B. WITKOP† AND E. X. ALBUQUERQUE*

* *Department of Pharmacology and Experimental Therapeutics, University of Maryland School of Medicine, Baltimore, Maryland 21201, and † Laboratory of Chemistry, National Institute of Arthritis, Metabolism and Digestive Diseases, Bethesda, Maryland 20014*

Received February 21, 1980; Accepted May 19, 1980

SUMMARY

SPIVAK, C. E., B. WITKOP AND E. X. ALBUQUERQUE. Anatoxin-a: A novel, potent agonist at the nicotinic receptor. *Mol. Pharmacol.* 18: 384–394 (1980).

Anatoxin-a, a semirigid, bicyclic amine, caused a depolarizing blockade of the indirectly elicited twitch in frog sartorius muscle. Concentration–response studies of contracture in the rectus abdominis and depolarization in the sartorius muscles of the frog showed that it is the most potent of the nicotinic agonists. It produced desensitization, and the kinetic and steady-state parameters found from chronically denervated rat soleus muscle were similar for anatoxin-a and acetylcholine. When endplate regions of frog sartorius fibers were voltage clamped, anatoxin-a induced endplate currents and concomitant increases in endplate current noise. Fourier analysis of this noise revealed that the average single channel lifetime was indistinguishable from that induced by acetylcholine; the single channel conductance was about 25% less for the toxin compared to acetylcholine. Analysis of nerve evoked endplate currents and spontaneous, miniature endplate currents indicated that the toxin did not alter the time constants for decay or the linearity of the current–voltage relationship. We conclude from this evidence that anatoxin-a does not block the open ion channel and does not produce a voltage-dependent blockade of the closed ion channel. The activity of this unusual agonist may be related to the coulombic and hydrogen bond free energies of binding to the receptor.

INTRODUCTION

Anatoxin-a (AnTX-a)[1] is an exotoxin isolated from a filamentous, freshwater, blue-green alga, *Anabaena flos-aquae*. Wind-blown concentrations of the algal surface blooms have killed livestock and waterfowl that ingest the water (1). The cause of death is respiratory paralysis (1), and the mode of action has the characteristics of a possible depolarizing neuromuscular blocking agent (1–3). AnTX-a is a bicyclic secondary amine (Fig. 1) whose structure has been determined by X-ray crystallography (4) and by spectroscopy (5); it has been synthesized from 1-methylpyrrole (6). Since it possesses no ester function, it is stable in the presence of acetylcholinesterase. Its bicyclic structure and conjugated ketone group severely restrict its conformational possibilities, making it one of the very few nearly rigid, potent nicotinic agonists.

The neuromuscular blockade by an agonist is the sum of two major, kinetically distinct processes that occur at the acetylcholine receptor, namely, membrane depolarization and desensitization. The amount of membrane depolarization depends on the identity of the agonist and its concentration at the synaptic cleft. Desensitization, a less understood phenomenon, involves a spontaneous recovery of membrane potential, despite the continued presence of the agonist, and decreasing responses to identical treatments by the agonist (7). The membrane depolarization is known to arise from the opening of cation channels that are activated after the agonist binds to the associated acetylcholine receptor. The channels conduct brief (about 1-ms duration), rectangular pulses of cationic current (about 2 pamp) that can be displayed directly by the single channel recording method (8) or can be characterized indirectly by the techniques of noise spectral analysis (e.g., 9–11) and voltage jump relaxation analysis (12). A noteworthy finding has been that channel properties, lifetime and conductance, are not fixed, but rather depend upon the identity of the agonist (e.g., 9). Though the reason for this is not known, an intuitive partial explanation, that the agonist remains bound to the receptor while the cation channel is open, is supported by indirect evidence (13, 14). The agonist, then, seems to be a key in the receptor–ion channel complex

This study was supported in part by United States Public Health Service Grant NS-12063 and by United States Army Research Office Grant DAAG 29-78-G-0203. The computer time for this project was supported in part through the facilities of the Computer Science Center of the University of Maryland.

[1] Abbreviations used: anatoxin-a, AnTX-a; acetylcholine, ACh; carbachol, carb; succinylcholine, SuCh; decamethonium, C10; miniature endplate potential, mepp; endplate current, epc; miniature endplate current, mepc.

0026-895X/80/060384-11$02.00/0

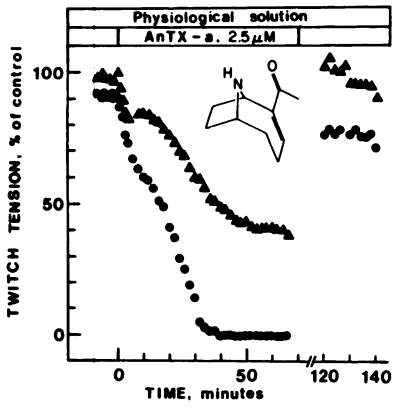

FIG. 1. *Paralysis of a frog's sartorius muscle by AnTX-a*

The direct (▲) and indirect (●) twitch tensions are plotted as a function of the time after applying AnTX-a (2.5 μM). The muscle was washed in normal frog Ringer's solution after a 20-min exposure to the AnTX-a solution, and the direct twitch returned to control levels within 50 min. The indirect twitch did not recover fully. The inset shows the structure of AnTX-a in the *s-trans* conformation.

that not only allows the bolt to move but also determines how far and how fast. The structural elements of the agonist that govern these movements are unknown.

The objectives of this research are to quantitate the agonist properties of AnTX-a and, as far as possible, to relate these to the fundamental elements of neuromuscular transmission. Of particular interest are the properties of the ion channel activated by AnTX-a. Though these properties are central to the depolarizing action, the relationship to molecular structure and to cleft concentration, governed by diffusion and enzymatic destruction, needs clarification. A suspected side reaction of the toxin was direct blockade of open ion channels. An agonist, decamethonium (15), and a classical competitive antagonist, *d*-tubocurarine (16), as well as a wide variety of structurally unrelated compounds (e.g., 17) seem to have this effect, and evidence that AnTX-a shares this property was sought.

The present study shows that AnTX-a is indeed a potent agonist at nicotinic acetylcholine receptors. It causes, at micromolar concentrations, blockade of frog sartorius muscle that is characterized by depolarization and repolarization (desensitization) of muscle fibers. Other measures of desensitization showed it to be similar in rate and equilibrium parameters to acetylcholine. Furthermore, AnTX-a activates the receptor ion channels to produce a channel lifetime indistinguishable from that produced by acetylcholine and a channel conductance that is about 25% less. No clear evidence that AnTX-a reacts with ionic channels in either closed or open conformation was found. Due to its apparently rigid structural architecture, AnTX-a does allow an in-depth stereochemical analysis of the ACh receptor recognition sites.

MATERIALS AND METHODS

Solutions and drugs. The frog Ringer solution had the following composition (mM): NaCl, 116; KCl, 2.0; $CaCl_2$, 1.8; Na_2HPO_4, 1.3; NaH_2PO_4, 0.7. For the glycerol shock treatment, 600 mmol of glycerol was added per liter of the above solution (18). To eliminate the appearance of action potentials and any local inward increase in sodium conductance, the intracellular recordings of membrane potential, desensitization (iontophoretic application of agonists), endplate current noise, and miniature endplate currents were made in the presence of tetrodotoxin (0.3 μM).

The rat Krebs Ringer solution had the following composition (mM): NaCl, 135; KCl, 5.0; $MgCl_2$, 1.0; $CaCl_2$, 2.0; $NaHCO_3$, 15.0; Na_2HPO_4, 1.0; and glucose, 11.0. The solution was bubbled continuously with 95% O_2, 5% CO_2, and the pH was 7.1–7.2. (±)-Anatoxin-a was stored under refrigeration as a 10 mM stock aqueous solution. Acetylcholine chloride, carbachol chloride, and tetrodotoxin were purchased from Sigma, and succinylcholine chloride was purchased from K & K Laboratories. The tetrodotoxin was stored under refrigeration as a 3×10^{-4} M stock solution. Purified α-bungarotoxin was obtained as a lyophilized solid from the Miami Serpentarium. Physiological solutions of all drugs and toxins used were freshly prepared on the day of use.

Animals and preparations. In most experiments isolated sartorius muscles, with or without the sciatic nerve, from the frog *Rana pipiens* were used at 21–23°C. Rectus abdominis muscles from *R. pipiens* were used for the contracture experiments. Chronically denervated (10–14 days) soleus muscles from Wistar strain rats were used in some desensitization experiments and to balance iontophoretic pipets (19). The muscles, removed under ether anesthesia, were used at 21–23°C. For muscle twitch and contracture experiments, muscles were mounted in an organ bath under 2–3 g resting tension and connected to a force displacement transducer. Muscle twitch was elicited directly and indirectly by supramaximal current pulses delivered at 0.05 Hz as that described elsewhere (20).

Electrophysiological techniques. For intracellular recording of the endplate region located on the surface fibers, muscles were stretched slightly over a planoconvex lens and pinned to a paraffin block. Recording microelectrodes were filled with 3 M KCl and had resistances between 3 and 5 MΩ. Impalement at the endplate region was assumed when the rise time of miniature endplate potentials was less than 1.0 ms. Iontophoretic application of drugs was delivered by microelectrodes containing 5M ACh, 2 M carbachol, or 10 mM AnTX-a as previously described (19). The recording and analysis of endplate noise were similar to those described previously (11, 19).

Endplate current experiments were performed on nerve–muscle preparations as described elsewhere (11, 14). The nerve was stimulated (four shocks per minute) during and after the glycerol treatment, which lasted 60 to 70 min. The muscle was then washed (about 6 ml/min) in normal frog Ringer's solution for an hour or more. The nerve, resting on bipolar platinum electrodes, was electrically insulated from the bulk solution with Dow Corning silicone stopcock grease. Supramaximal stimulation of the nerve was achieved by delivering 4- to 8-V pulses of 0.05-ms duration to the platinum electrodes. Data from these experiments were sent, on line, for storage and analysis by a PDP 11/40 computer (Digital Equipment Corp., Marlboro, Mass.). Digitized endplate

current (epc) points were sampled at 100-μs intervals, and the logarithms of the decay values decreased linearly with time. The epc decay time constants (τ_{epc}) were determined by the computer from the linear regression analysis of these plots. Only the middle 60% of the decay was used to evaluate the τ_{epc}. The calculated τ_{epc} and peak amplitude values were rejected if the clamp error exceeded 5% of the command potential.

The command potential of the fibers used for the epc experiments was changed in 10-mV steps of 3-s duration, starting at −50 mV and proceeding in the depolarizing direction first. In this way each cell yielded a family of epcs from which were derived one complete current–voltage plot and one plot of logarithm τ_{epc} versus membrane potential.

Miniature endplate currents. Recording proceeded as in the noise experiments. On playback of the tape, mepcs were captured on a Gould OS4000 digital storage oscilloscope and sent to the computer. To smooth the ripple of noise in the records, many digitized mepcs were averaged at each sampled time point in the decay phase, and the logarithms of these averages were plotted against time. Linear regression analysis of these plots provided estimates of the mepc decay-time constant.

RESULTS

The effect of AnTX-a on isolated skeletal muscle preparations. The addition of AnTX-a to the organ bath produced neuromuscular blockade of the directly and indirectly elicited twitch of the frog sartorius muscle. At concentrations of 2.5 μM and greater, AnTX-a abolished the indirect twitch of frog sartorius muscle preparations (Fig. 1). The rate at which the blockade developed increased with the concentration, taking about 40 min for complete blockade at 2.5 μM and about 10 min at 10 μM. Suppression of the directly elicited twitch was seen, and this was probably due to the effect of AnTX-a on the action potential, discussed later. This effect on the direct twitch was reversible upon washing for 1 h, though the indirect twitch showed incomplete recovery.

More quantitative experiments resulted from comparing the contractile response of the frog's rectus abdominis muscle during exposure to AnTX-a, carbamylcholine, or succinylcholine. Desensitization of the junctional ACh receptor, which took as long as 45 min to reverse, limited the amount of data that could be obtained from a single muscle and required pooling data from three to five muscles. The results of these compiled experimental data are shown in Fig. 2. These data show that there are no significant differences among the slopes of the linear regression lines, that the relative potency of AnTX-a to carbamylcholine is about 12:1, and that the relative potency of AnTX-a to succinylcholine is about 10:1 in this muscle. These ratios were supported by direct comparisons of the drug responses on individual muscles (not shown).

The effect of AnTX-a on muscle membrane potential. Intracellular recording showed that AnTX-a reacted with the ACh receptor as a typical agonist at the frog neuromuscular junction. AnTX-a produced a membrane depolarization of the muscle endplate followed by spontaneous repolarization on prolonged treatment (Fig. 3).

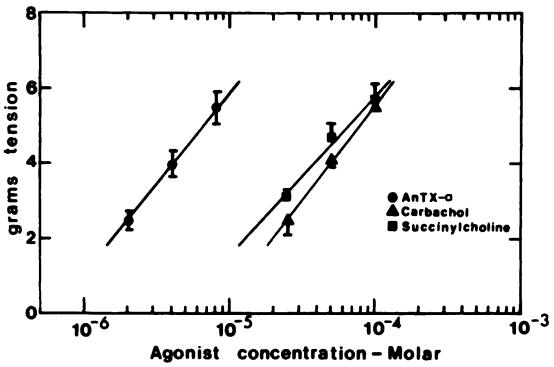

FIG. 2. *Comparison of AnTX-a, carbachol, and succinylcholine concentration–response curves on the frog's rectus abdominus muscle*

Each symbol represents the mean ± SE contracture tension obtained at each concentration of agonist used. The slopes of the linear regression lines (±SD of the slope) and the estimated concentrations for a 4-g response are: AnTX-a, 4.9 ± 0.8 g, 4 μM; carb, 5.1 ± 0.6 g, 49 μM; SuCh, 4.2 ± 0.8 g, 38 μM.

This is an effect also seen with the typical nicotinic agonists, acetylcholine, decamethonium, nicotine, carbachol, and succinylcholine (21–24). The progress of this action can be monitored by recording continuously from a single cell (Fig. 3A) or by sampling many cells through time (Fig. 3B). Although the former method yielded more homogeneous data (Fig. 3A), it may suffer from a small,

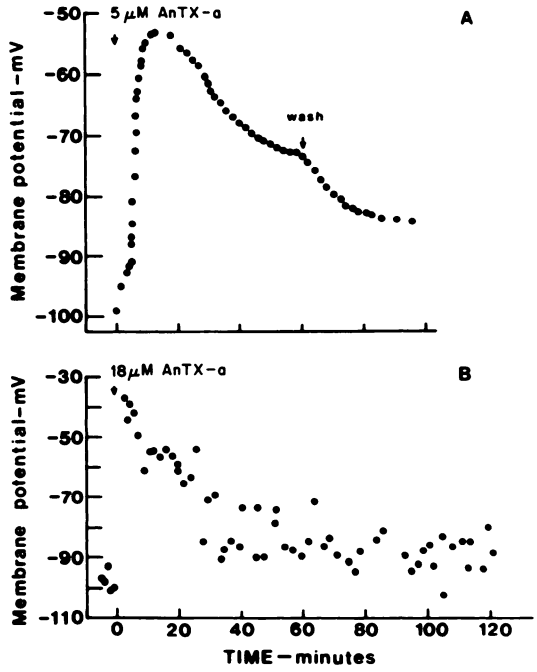

FIG. 3. *Intracellular recording of sartorius fibers in the presence of AnTX-a*

A shows the membrane potential of a single endplate recorded continuously before, during, and after the addition of AnTX-a (5×10^{-6} M) to the bath. The drug was added and removed by continuous superfusion of the muscle with the indicated solution. In B each symbol represents a different fiber from one muscle. At the time indicated (0 min), the bath was drained and refilled with frog Ringer's solution containing 1.8×10^{-5} M AnTX-a. Following rapid depolarization the fibers spontaneously repolarized despite continued presence of the drug. No wash is shown in B.

systematic error that overestimates the membrane depolarization because of cell damage. Thus, only results from the second method of recording were averaged for Fig. 4A. This method showed that the AnTX-a effect was reversible, since membrane potentials returned to control values after washing. During the onset of depolarization miniature endplate potentials (mepps) disappeared, usually within the first 1–4 min in the drug solution, when membrane potentials were between −60 and −70 mV. The mepps were found to return after washing the muscle for about 12 min or more and when the membrane potential had repolarized to about −70 mV and greater. Carbachol, at about 10-fold higher concentrations, showed similar effects.

The rate of receptor desensitization was estimated from the rate of membrane repolarization. Figure 3 and other results obtained from suitably high AnTX-a concentrations showed that desensitization proceeded by an approximately exponential time course, but the rate at low AnTX-a concentrations was so slow that only a linear phase of repolarization could be measured. To accommodate all the data, only the slopes of the most nearly linear parts of the curves were taken as estimates of the rate of desensitization, and these are plotted in Fig. 4B.

The process of desensitization caused by AnTX-a. Experiments similar to those of Katz and Thesleff (7) were performed using double-barreled pipets on the junctional region of the frog sartorius or the chronically denervated rat soleus muscles. Typical responses obtained by microiontophoretic application of AnTX-a at the denervated rat soleus muscle are shown in Fig. 5 (inset). Frog fibers gave similar responses. A steady depolarization was produced by AnTX-a released from one barrel of the pipet while short test pulses of AnTX-a were delivered by the other barrel. The amplitude of the test pulses varied with time both during and after the steady AnTX-a release according to the function

$$V = V_0 e^{-Rt} + V_1,$$

where V_0 is negative for the recovery phase. The parameters were evaluated by nonlinear regression analysis (25), and the rate constants thus calculated showed no significant dependence on the extent of membrane de-

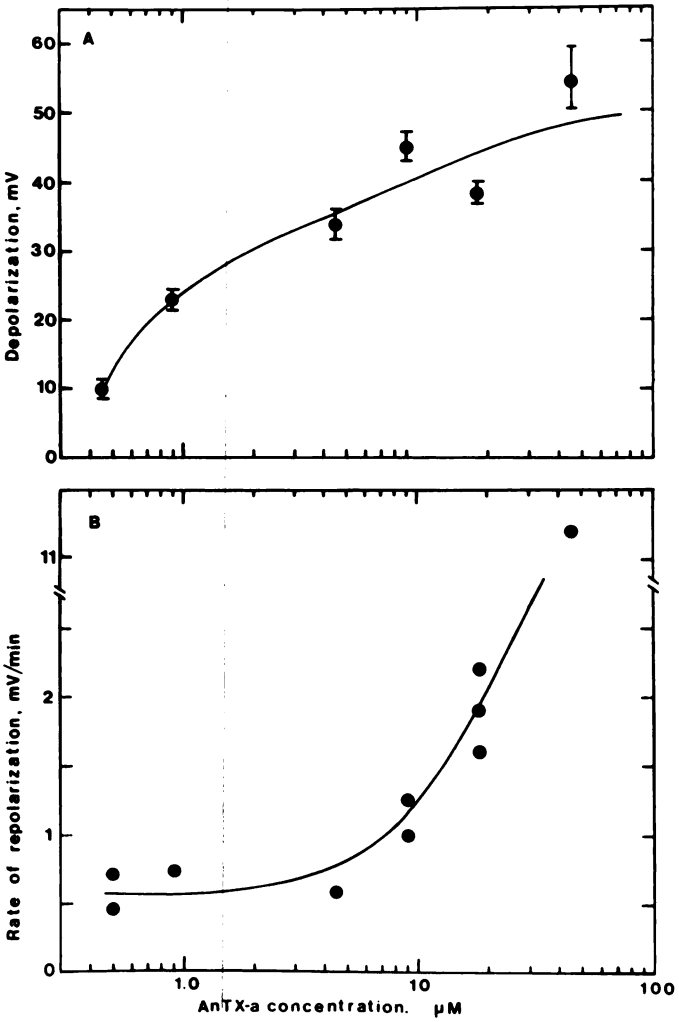

FIG. 4. *Maximum depolarization and rate of spontaneous repolarization for sartorius endplates in the presence of bath-applied AnTX-a at various concentrations*

Each symbol in A except the one at 4.5×10^{-5} M represents the mean ± SE from 19 to 34 fibers recorded from three to five muscles. Usually the maximum of depolarization, defined here as the difference between the membrane potential at the peak of depolarization and the average control membrane potential (usually about −95 mV) sampled before the addition of the agonist, was sufficiently protracted that several fibers could be recorded at the peak. At 4.5×10^{-5} M AnTX-a, however, repolarization was so rapid that only one fiber from each of three muscles appeared to be at the peak, and only these were averaged (see Fig. 4B). The rate of spontaneous repolarization is shown in B as a function of the AnTX-a concentration. Each symbol represents the slope (fitted by eye) of the most linear part of the repolarization curve from one experiment.

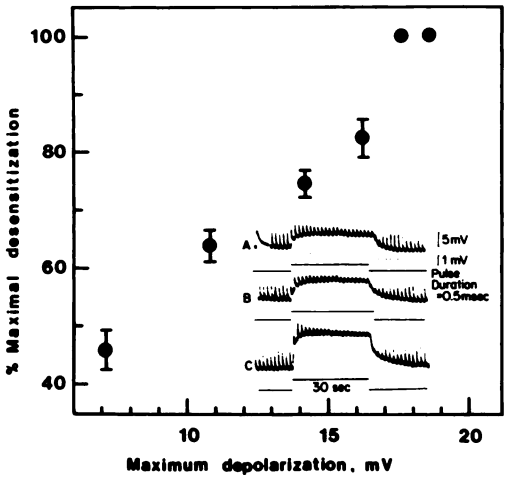

FIG. 5. *Steady-state desensitization of a frog sartorius fiber by AnTX-a*

The percentage maximal desensitization, defined in the text, was derived from the nonlinear regression parameters for an exponential function. Each point is the result of a single trial. The standard error bars shown were estimated by the deviation of the test pulse amplitudes from the exponential function. The inset shows examples of the experimental results. The sawtooth-like trace (top in each series) is the fiber response to the iontophoretic potentials (across a 50-kΩ resistance) shown in the second and third traces of each series. The first response in A was recorded on an expanded (10X) time scale. The responses shown in B and C are from the same fiber as in A, only the extent of steady membrane depolarization differed.

polarization. The time constants ($1/R$) obtained from frog sartorius fibers (mean value of eight responses sampled from three muscles) were 15 ± 3 (SE) s for the onset and 16 ± 2 s for the offset of receptor desensitization. One tendency seen was that onset of desensitization seemed faster than offset at lower responses and vice versa at the higher responses. This is in qualitative agreement with the cyclic mechanism for desensitization proposed by Katz and Thesleff (7). When the percentage of desensitization (at infinite time), defined as $D = 100\{1 - [V_1/(V_0 + V_1)]\}$, was plotted against the maximum depolarization, the linear relationship, seen in Fig. 5, resulted. Though tempted, one cannot combine the AnTX-a concentration vs membrane depolarization data with the desensitization vs membrane depolarization data to produce a plot of desensitization vs AnTX-a concentration. This is because the AnTX-a released by microiontrophoresis acts at widely varying concentrations along the length of the endplate (see, for example, 26), and the membrane depolarization thus seen is at best an average that does not take into account the nonlinearity of the concentration–response curve.

Another experiment directly compared the membrane desensitizing action of acetylcholine with AnTX-a at two fibers from a chronically denervated (11 days) rat soleus muscle. Both steady depolarization and test pulsing were achieved by rapid (16-Hz) microiontophoretic pulses applied from one barrel of the double-barreled pipet. The two barrels contained AnTX-a and acetylcholine, respectively. Again, nonlinear regression analysis found estimates for the parameters, assuming a single exponential plus a constant as before. The time constants for onset of desensitization, 3.4 ± 0.5 s ($N = 3$) for ACh and 2.6 ± 0.3 s ($N = 3$) for AnTX-a, were indistinguishable for these two agonists. The maximum percentage of desensitization, defined as $100[1 - (V_1/V_{max})]$, is plotted in Fig. 6. The important feature of this graph is that no difference between ACh and AnTX-a can be seen. The observation that both AnTX-a and acetylcholine, upon direct comparison, showed similar rate and equilibrium (or steady-state) parameters for desensitization suggests that the fundamental equilibrium and rate constants that determine these effects are similar for these two drugs.

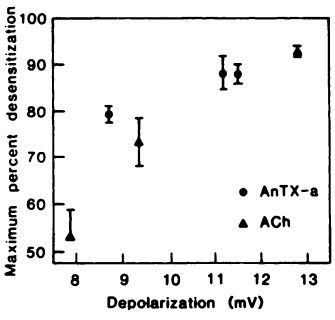

FIG. 6. *Steady-state desensitization of a chronically denervated rat soleus fiber by AnTX-a and acetylcholine*

By using rapid microiontophoretic pulses and a double-barreled pipet, it was possible to compare these two agonists directly in the same experiment. Acetylcholine was contained in one barrel of the pipet, and AnTX-a in the other. Each symbol, the result of a single test, was derived from the nonlinear regression parameters, as described in the text. The standard error bars were estimated from deviations of the test pulse amplitudes from an exponential function. These results come from two fibers of one muscle.

Action potentials. Carbachol diminishes the rate of rise, amplitude, and overshoot of the muscle action potential, and it prolongs the half-decay time (22). We wanted to know if AnTX-a had similar actions and whether AnTX-a acts directly on the voltage-sensitive cation channels. Figure 7A shows typical action potentials before, during, and after AnTX-a (2 μM) treatment. AnTX-a consistently altered action potential properties in the same ways as does carbachol. Like carbachol, AnTX-a did not affect threshold. To determine if this AnTX-a action was exerted via the ACh receptors, the latter were blocked by a supersaturating amount of α-bungarotoxin (5 μg/ml, 1 h; wash 1 h) before the experiment was repeated. This time (Fig. 7B) the action potentials were unaltered by AnTX-a, implying that AnTX-a, at 2 μM, had no direct effect on the Na^+ and K^+ channels.

Single channel properties. Voltage-clamped frog sartorius fibers responded to microiontophoretic application of AnTX-a or acetylcholine with a voltage-dependent response of endplate currents, samples of which are shown in the top traces of Fig. 8. These same records, seen at higher gain and filtered in the second traces from

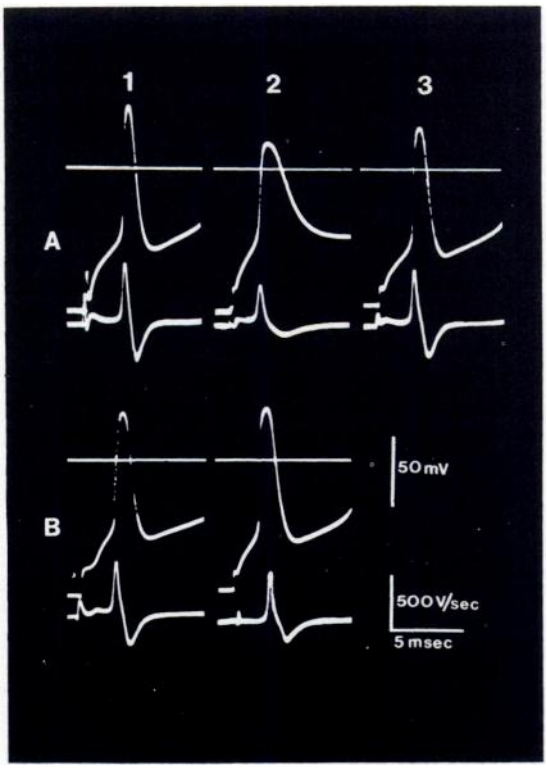

FIG. 7. *The effect of AnTX-a on action potentials elicited in frog sartorius fibers*

Typical control action potentials are shown in column 1. Column 2 shows action potentials elicited during treatment with 2×10^{-6} M AnTX-a for 40 min (A) or 80 min (B). In B, however, the muscle had been saturated with α-bungarotoxin and washed before adding AnTX-a to the bath. When the muscle was washed (>2 h here, column 3), the action potential approached control. All records are from nonjunctional regions. The membrane potential in A2 was −45 mV. All membrane potentials were raised to −90 or −100 mV by a second, current-passing microelectrode.

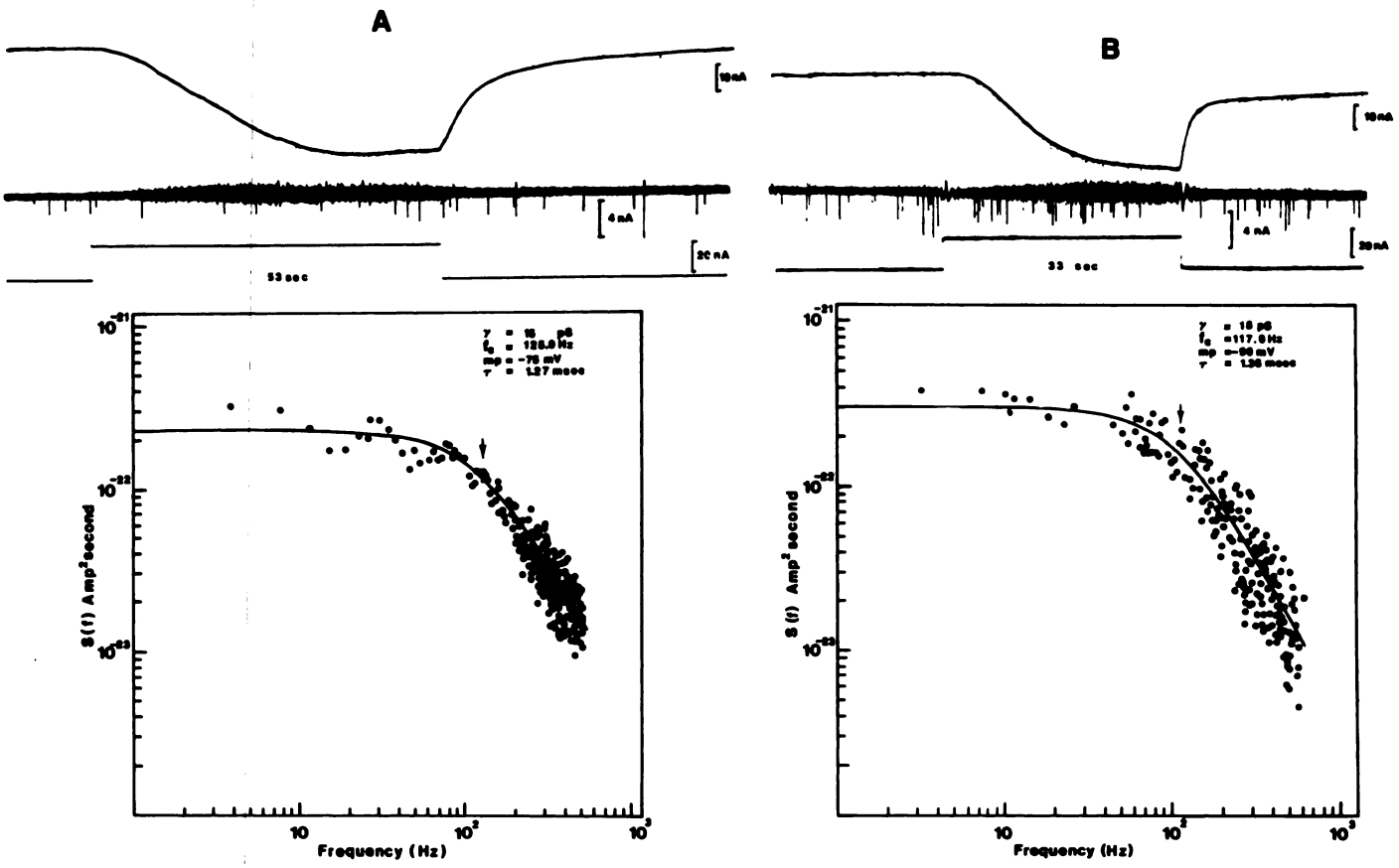

FIG. 8. *Endplate current noise and its power density spectra for AnTX-a (A) and acetylcholine (B)*

Total, DC coupled endplate currents, top traces, are shown amplified and filtered in the second traces, where the increased endplate noise can be seen. The sharp downward deflections are miniature endplate currents. The microiontophoretic currents are shown in the third traces. The plateau regions of the endplate currents were subjected to Fourier analysis to produce the power density spectra shown. Cutoff frequencies (fc) are indicated by the arrows. The solid lines are Lorentzian functions fitted to the analysis points by a least-squares method. Average single channel lifetimes (τ_I) and conductances (γ) as well as cutoff frequencies and membrane potentials are shown in each plot.

the top, show the enhanced endplate noise that results from the random opening of the elementary ion channels. Fourier analysis of the noise yields the power density spectra shown at the bottom of the figure. The spectra obtained were Lorentzian in shape, as expected for one class of independent channels that open and close according to a first-order kinetic reaction (10); more complicated spectra were not seen. These spectra yielded values for average channel lifetime, τ_I, and channel conductance, γ.

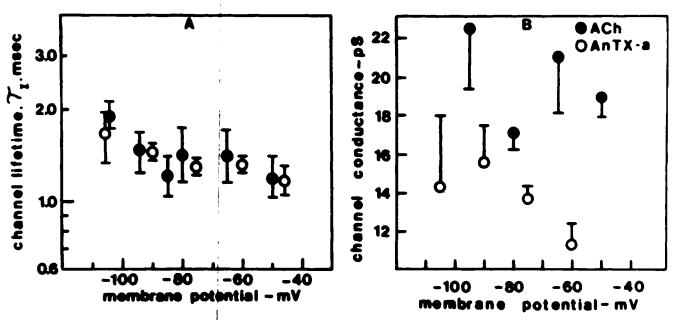

FIG. 9. *Average single channel lifetime (A) and conductance (B) at various membrane potentials for AnTX-a and acetylcholine*

Each symbol represents the mean ± SE usually from 5 to 10 spectral analyses and four (acetylcholine) or six (AnTX-a) experiments.

Channel lifetimes are plotted against membrane potential in Fig. 9A. A tendency toward the expected dependence on voltage (e.g., 10) is seen over this narrow range of potentials. There is no difference between channel lifetime induced by AnTX-a and by acetylcholine at any given membrane potential. This conclusion is confirmed in Table 1, which shows the results of paired responses obtained from the same fiber as described below.

Averaged values of channel conductance from several noise experiments are shown in Fig. 9B, in which AnTX-a is compared to acetylcholine. The difference found at each membrane potential was highly significant based on Student's t test ($P < 0.01$). To confirm this result, however, the two agonists were compared directly. Double-barreled pipets, containing acetylcholine in one barrel and AnTX-a in the other, were positioned above a voltage-clamped muscle fiber. Only consecutive, paired responses, obtained at the same fiber clamped at the same potential were compared. The paired total endplate current responses were usually within a factor or two of each other. The paired differences in τ_I and γ for two experiments are shown in Table 1. This experimental design incorporated the most direct method available for comparing the two drugs, and it showed that the acetylcholine γ may be slightly larger, probably by about 25%, than the AnTX-a γ.

TABLE 1

Ion channel properties from paired responses to AnTX-a and ACh

The agonists, contained in a double-barreled pipet, were delivered by microiontophoresis as a pair of successive tests to a fiber. The differences in channel properties (AnTX-a minus ACh), found from noise analysis, are shown. The mean differences and their standard errors indicate that channel lifetimes are indistinguishable for AnTX-a and ACh, but that channel conductances do differ significantly.

Pair code	Membrane potential	Channel lifetime (ms)			Channel conductance (pS)		
		AnTX-a	ACh	Difference	AnTX-a	ACh	Difference
	mV						
66-20	−45	0.85	0.94	−0.09	11.8	15.9	−4.1
66-2L	−55	1.26	0.88	0.38	9.4	19.8	−10.4
21-2M	−55	1.26	1.72	−0.46	14.6	19.6	−5.0
21-2J	−65	1.54	1.54	0.00	13.2	17.2	−4.0
21-2D	−75	1.29	2.55	−1.26	15.1	16.0	−0.9
21-2F	−75	—	—	—	15.8	16.5	−0.7
66-2B	−80	1.00	0.94	0.06	10.2	15.0	−4.8
21-2H	−85	1.81	1.74	0.07	13.6	13.9	−0.3
66-2I	−95	1.50	1.25	0.25	9.9	17.3	−7.4
			Mean	−0.13		Mean	−4.2
			SE	0.18		SE	1.11*

* $P < 0.01$.

AnTX-a increases mepc frequency. During these experiments a presynaptic effect was seen. The iontophoretic release of AnTX-a induced on several occasions a dramatic increase in the miniature endplate current frequency (Fig. 10). In nine records (four muscles) that showed this effect, the ratio of maximum mepc frequency (averaged over 10 or 20 s) to frequency before application of AnTX-a was 12.6 ± 1.6 (SE). This value may be underestimated due to the difficulty of distinguishing mepcs from the heightened endplate current noise response. Upon recovery from the iontophoretic AnTX-a application, the mepc frequency returned to control values. This finding contrasts with that of Duncan and Publicover (27), who presented evidence of a presynaptic muscarinic receptor at the frog cutaneous pectoris neuromuscular junction that inhibits transmitter release. AnTX-a had a weak muscarinic action compared to acetylcholine at the guinea pig ileum (3). Moreover, AnTX-a binds with >1000-fold higher affinity to nicotinic receptors than to muscarinic ones (28).

Kinetics of off response to iontophoretic AnTX-a application. When the iontophoretic current was discontinued, the endplate current recovered in a double exponential manner. This can be seen in the top traces of Fig. 8, for example. We investigated this quantitatively to see if AnTX-a was held up in any compartment not accessible to quaternary amine agonists. A semilogarithmic plot of this decay is shown in Fig. 11A, in which successive, paired responses to acetylcholine and AnTX-a, released by a double-barrel pipet exactly as in the noise experiments, are compared. The fast phases were seen to be almost parallel, but the slow phases had distinctly different slopes. Similar direct comparisons were conducted between carbachol and AnTX-a, but, as seen in the example in Fig. 11B, no such differences were found. The decay rate constants were evaluated by nonlinear regression analysis (25), and their mean ratios (±SE) for four pairs of tests were as follows: AnTX-a:carb (fast), 0.86 ± 0.21; AnTX-a:carb (slow), 0.98 ± 0.13; AnTX-a:ACh (fast), 0.87 ± 0.14; and AnTX-a:ACh (slow), 0.55 ± 0.09. Only the last ratio differs significantly (Student's t test, $P < 0.02$) from unity. Thus two kinetic compartments can be distinguished, but not enough information was available to decide which compartment held the ACh receptor and which held the acetylcholinesterase. No additional compartment for AnTX-a (a hydrophobic one, for example) was evident on the time scale of these experiments.

Effect of AnTX-a on endplate currents. Apart from its direct effect in activating the receptor–ion channel complex, it seemed a strong possibility that AnTX-a may also cause a blockade of the ion channel (see the Introduction). This action is often revealed in the neuronally evoked endplate currents (epcs) and in the spontaneous miniature endplate currents (mepcs) of voltage-clamped frog sartorius fibers. Signs of the channel blockade commonly seen are deviations from linearity of current–voltage relationships or alterations in the time course of the epc or mepc decay phase (e.g., see 11, 14, 17). The maximum AnTX-a concentration that could be used was about 0.9 μM. Above this concentration the epc amplitudes were so depressed that measurements were unreliable. This depression seemed to progress slowly with time during the 1–2 h of recording in the presence of AnTX-a and probably represented a dropout of receptors due to desensitization. The mean peak amplitudes from several fibers are plotted against the membrane potential in Fig. 12. AnTX-a causes a marked depression of the epc peak amplitude relationship; however, no difference in the form of the curves (linear) or in the null potentials (near 0 mV) was observed. The epc rise times, which averaged 0.8 ms, were unchanged by AnTX-a. The time course of the epc decays followed a single exponential function both in the absence and in the presence of AnTX-a. The time constants are plotted in Fig. 13 against the membrane potential. AnTX-a (0.9 μM) had no effect on the voltage sensitivity of the epc time constants. At each membrane potential the difference in τ_{epc} caused by AnTX-a was not significant. A hint of depression in τ_{epc} values by AnTX-a is seen in Fig. 13, but this change, if even significant, is small compared to the more striking changes caused by some other agents (e.g., see 11, 14, 17). It is possible that higher concentrations of AnTX-a would have enhanced the effect, but the technical difficulties mentioned earlier precluded these tests by the epc method. To further the search for an effect of AnTX-a on open ion channels, the decay phases of miniature endplate currents were examined.

The effect of AnTX-a on the mepc time course. The AnTX-a was delivered to voltage-clamped frog sartorius fibers by bath application or by microiontophoresis. In all experiments the spontaneous mepcs were recorded on tape before and during AnTX-a application. To smooth the ripple in the decay phase, all mepcs of a given condition were averaged by the computer at 0.056-s intervals after the peak. The τ_{mepc} value was obtained from linear regression analysis (see Materials and Methods).

Figure 14 shows the semilogarithmic plot of 17 control mepc decays and 16 mepc decays from the same cell in the presence of 1.8 μM bath-applied AnTX-a. The holding potential was −80 mV. Both averaged decays were exponential and have similar τ_{mepc} values, namely, 1.2 ms.

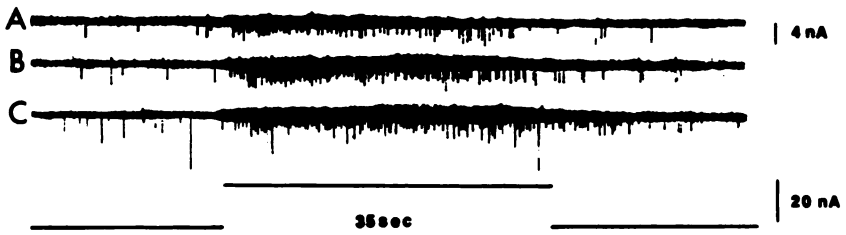

FIG. 10. *Increased mepc frequency produced by microiontophoretic application of AnTX-a*
The microiontophoretic application of AnTX-a, shown in the bottom trace, greatly enhanced the frequency of mepcs, shown as the sharp downward deflections in A, B, and C.

Two other experiments, one using 1.8 μM AnTX-a and the other using 0.9 μM AnTX-a, gave similar results. In another series of experiments the mepcs were averaged the same way before and during a microiontophoretic application of AnTX-a to yield a pair of averaged mepc decays for each test. A minimum of 5 mepcs was averaged under each condition, and 11 such pairs (157 mepcs, total), at holding potentials ranging from −70 to −100 mV, were compared. The average difference between pairs, 0.12 ± 0.09 (SE) ms, was judged to be insignificant (paired *t* test), thereby supporting the view that AnTX-a does not block open channels at concentrations that produce steady, moderate endplate currents.

DISCUSSION

The present results demonstrated that the novel agonist AnTX-a specifically reacted with the ACh receptor and was devoid of a significant effect on its ionic channel. This powerful agonistic action of AnTX-a on the neuromuscular synapse confirmed earlier studies (1–3) that this toxin caused depolarization of the junctional membrane. Indeed, AnTX-a causes all the typical qualitative phenomena, i.e., neuromuscular blockade (of the depolarizing type), contracture of the frog's rectus abdominis muscle, depolarization of the frog sartorius muscle, desensitization, and alteration of the action potential. It produced steady endplate currents that yielded estimates of the mean channel lifetime and channel conductance, and seemed to react with neither the closed nor the open conformations of the ion channels to reduce the channel lifetime. In addition, AnTX-a may have some presynaptic activity leading to an increase in mepc frequency.

The potencies of six nicotinic agonists are compared (Table 2) for their ability to depolarize the frog's sartorius muscle by 10 mV. Interpolations from data published by other authors are cited to show that *AnTX-a is the most potent of these six agonists.* This potency may be broken down into terms that express affinity to the receptor (i.e., dissociation constant(s)) and a term to express efficacy. For example, one of the simplest schemes is as follows:

$$A + R \underset{k_{-1}}{\overset{k_1}{\rightleftharpoons}} AR \underset{k_{-2}}{\overset{k_2}{\rightleftharpoons}} AR^*. \qquad [1]$$

Here, R is the unoccupied receptor, A is the agonist, and AR* is the activated (conducting) agonist–receptor com-

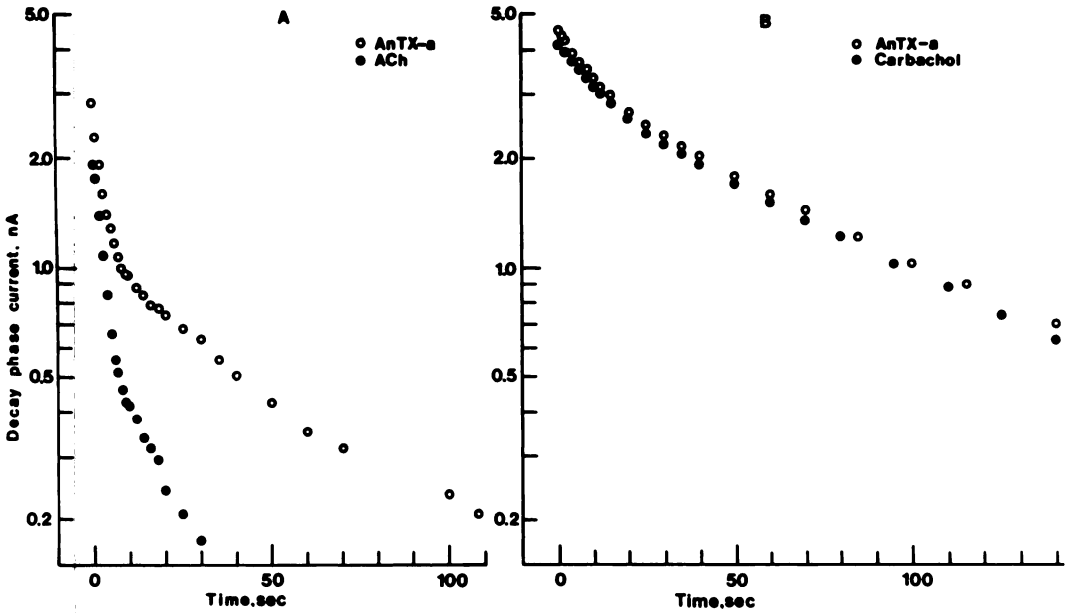

FIG. 11. *The temporal decrease in endplate current after cessation of the microiontophoretic current*
The agonists were delivered from double-barreled pipets to elicit paired responses (see text). The endplate currents show a biphasic decline in these semilogarithmic plots. Though AnTX-a and carbachol were similar in their kinetics, acetylcholine showed a faster rate of decline in the second phase.

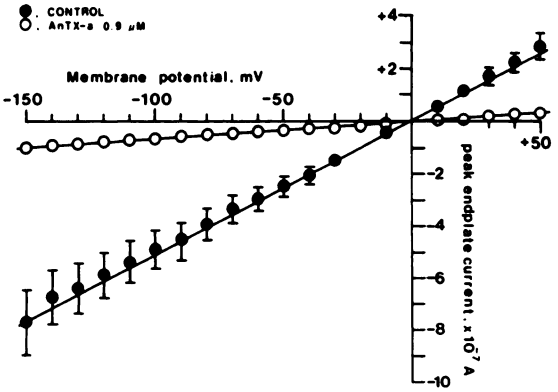

FIG. 12. *The effect of AnTX-a on the epc peak amplitude current-voltage relationship*

Each symbol represents the mean ± SE of 15–21 fibers at negative potentials and 4–13 fibers at positive potentials. The absence of a bar indicates that the SE was too small to be shown. AnTX-a markedly decreased the slope conductance without affecting its linearity or the null potential.

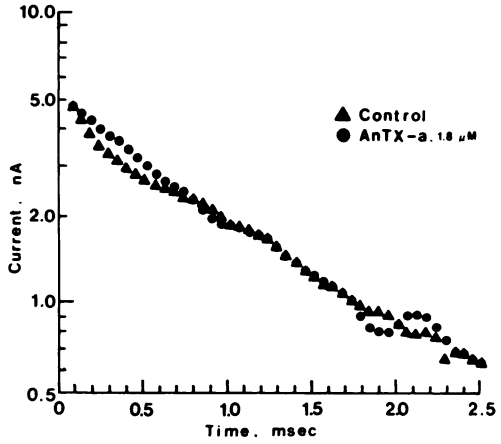

FIG. 14. *The effect of AnTX-a on mepc decays*

The averaged decays of 17 mepcs under control conditions and of 16 mepcs from the same fiber in the AnTX-a Ringer's solution are shown. No difference in the time constants for decay could be discerned.

plex, which represents the primary physiological response. In this case, as in more complicated models (see, e.g., 26), efficacy is a function of k_2, k_{-2}, and γ, the single channel conductance. Other parameters depend on the response that is measured, which may be many steps removed from the primary event. The rate constant k_{-2} in the scheme above is related to the average channel lifetime (at low agonist concentrations) by $k_{-2} = 1/\tau_I$ (10), where τ_I is the value obtained from endplate noise analysis. The τ_I value for AnTX-a is the same as that for acetylcholine and higher than that of any other agonist tested except for suberyldicholine (e.g., see 9). The γ value for AnTX-a was about 25% lower than that of acetylcholine. The evaluation of k_2 requires, inter alia, concentration–endplate current experiments, in progress, that may help to formulate the appropriate model for agonist binding and receptor activation.

Desensitization may limit the apparent potency of an agonist, especially at high agonist concentrations. Indeed, as shown in Fig. 3B, for example, within 30 s after the addition of AnTX-a to the experimental chamber, the first cell impaled at the junctional region displayed a peak depolarization which was rapidly superseded by a slower repolarizing or desensitizing phase. These two actions of AnTX-a probably account for the absence of a clear plateau in the concentration–depolarization curve of the agonist (Fig. 4A).

We have used two measures for the rate of desensitization. One was the rate of spontaneous repolarization of frog sartorius fibers during bath application of the agonist. The extent of membrane depolarization is not a linear function of the number of conducting channels (34) and, used without correction, is not a good measure of either agonist effect or desensitization. Depolarization is further complicated by relatively slow shifts in chloride ion concentration (32). The second method for measuring desensitization involves iontophoretic drug application and test pulses (7). The latter method, which did not produce depolarization great enough to require correction for nonlinear summation, showed that AnTX-a desensitized a chronically denervated rat soleus muscle at the same rate as did acetylcholine, and that the maximum

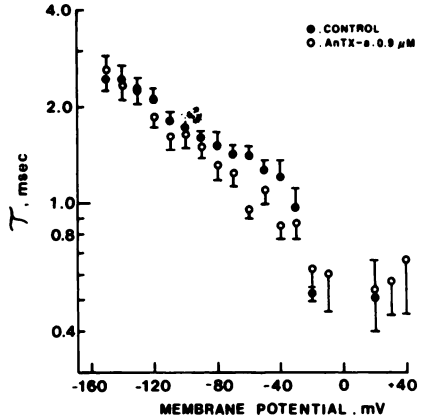

FIG. 13. *The effect of AnTX-a on the epc decay time constants*

Each symbol represents the mean ± SE for four to eight fibers at membrane potentials more negative than −10 mV or for two or three fibers at the other potentials.

TABLE 2

Concentrations of various agonists that produce 10-mV depolarization in frog sartorius muscle

Concentration	Agonist	Reference
μM		
0.2[a]	AnTX-a	(2)
0.4	AnTX-a	Present results
1[b]	ACh	(29)
3	SuCh	(24)
6	Carb	(31)
9[a]	C10	(2)
10	Carb	(33)
12	Carb	(32)
15	Nic	(30)
20	Nic	(23)
20	C10	(24)
80	C10	(33)

[a] Assumes control membrane potential of −85 mV.

[b] 10^{-5} M Physostigmine present; recording begun 10–15 min after adding ACh to the bath.

(steady-state) desensitizations produced by the two agonists were also similar (see Fig. 6). Thus, regardless of the mechanism, the various rate constants involved are similar for AnTX-a and ACh. More thorough experiments are in progress.

A third limitation of potency may arise from the agonist's ability to block the channel as well as to activate it. Decamethonium may be an example (15). The variety of compounds apparently capable of blocking the ion channel in open and in closed conformations (see 11, 13, 14, 16, 17) prompted a search for such actions by AnTX-a. Since AnTX-a did not alter the exponential character of either epc or mepc decays, the time constants of these decays, and the linear voltage dependence of the epc peak amplitudes, it can be concluded that, at physiologically active concentrations, the toxin does not oppose its own agonist action at the recognition site with channel blocking actions somewhere else.

The relationship between the structure of an agonist and its potency is not clear at the nicotinic receptor. It is likely that a number of factors contribute in different ways. The initial bond between the agonist and the receptor is probably electrostatic, the energy of which depends inversely upon the distance between the center of positive charge in the agonist and the anionic site of the receptor. Anatoxin-a has the unusual advantage of being a secondary amine, and it can therefore achieve a stronger coulombic bond than can the bulkier quaternary amine agonists. Further stability ensues when a postulated hydrogen bond forms, and the facility of this reaction depends on the geometric relationship between the center of positive charge and the hydrogen bond acceptor in the agonist molecule (35). Anatoxin-a has the advantage over most agonists in that its possible conformations are essentially restricted to the *s-cis* and the *s-trans* rotamers of the planar, conjugated system, O═C—C═C. The *s-cis* (but not the *s-trans*) conformation fits the geometric model of Beers and Reich (35) nicely and is likely to be the one that activates the receptor.[2] The importance of the planar restriction is suggested by the report (6) that dihydroanatoxin-a is only one-tenth as toxic in mice (ip injection) as is AnTX-a. Other aspects of structure–action relationships at the nicotinic receptor remain to be clarified. Anatoxin-a, with its highly restrained structure, and its analogues may become important tools in elucidating the molecular details for receptor activation and desensitization.

ACKNOWLEDGMENTS

We are grateful to Dr. Regina Marcus and to Mr. Aaron Rapoport for assistance in the depolarization and contracture experiments, respectively. The expert computer analysis and general technical assistance of Ms. Mabel Alice Zelle are greatly appreciated. We thank Dr. Michael Epstein for critical review of the manuscript.

[2] The infrared absorption bands for C═C at 1645 (weak) and 1588 (medium) cm^{-1} (5) suggest that a considerable proportion of AnTX-a·HCl exists as the *s-cis* conformation in $CHCl_3$ solution (36). The *N*-acetyl derivative of AnTX-a crystallizes in the *s-trans* conformation (4).

REFERENCES

1. Carmichael, W. W., D. F. Biggs and P. R. Gorham. Toxicology and pharmacological action of *anabaena flos-aquae* toxin. *Science* **187:** 542–544 (1975).
2. Biggs, D. F., and W. F. Dryden. Action of anatoxin-I at neuromuscular junction. *Proc. West. Pharmacol. Soc.* **20:** 461–466 (1977).
3. Carmichael, W. W., D. F. Biggs and M. A. Peterson. Pharmacology of anatoxin-a, produced by the freshwater cyanophyte *anabaena flos-aquae* NRC-44-1. *Toxicon* **17:** 229–236 (1979).
4. Huber, C. S. The crystal structure and absolute configuration of 2,9-diacetyl-9-azabicyclo[4,2,1]non-2,3,-ene. *Acta Crystallogr. Ser. B* **28:** 2577–2582 (1972).
5. Devlin, J. P., E. O. Edwards, P. R. Gorham, N. R. Hunter, R. K. Pike and B. Stavric. Anatoxin-a, a toxic alkaloid from *Anabaena flos-aquae* NRC-44h. *Canad. J. Chem.* **55:** 1367–1371 (1977).
6. Bates, H. A., and H. Rapoport. Synthesis of anatoxin-a via intramolecular cyclization of iminium salts. *J. Amer. Chem. Soc.* **101:** 1259–1265 (1979).
7. Katz, B., and S. Thesleff. A study of the 'desensitization' produced by acetylcholine at the motor end-plate. *J. Physiol. (London)* **138:** 63–80 (1957).
8. Neher, E., and B. Sakmann. Single channel currents recorded from membrane of denervated frog muscle fibers. *Nature* **260:** 799–801 (1976).
9. Katz, B., and R. Miledi. The characteristics of 'end-plate noise' produced by different depolarizing drugs. *J. Physiol. (London)* **230:** 707–717 (1973).
10. Anderson, C. R., and C. F. Stevens. Voltage clamp analysis of acetylcholine produced end-plate current fluctuations at frog neuromuscular junction. *J. Physiol. (London)* **235:** 655–691 (1973).
11. Adler, M., A. C. Oliveira, E. X. Albuquerque, N. A. Mansour and A. T. Eldefrawi. Reaction of tetraethylammonium with the open and closed conformations of the acetylcholine receptor ion channel complex. *J. Gen. Physiol.* **74:** 129–152 (1979).
12. Adams, P. R. Relaxation experiments using bath-applied suberyldicholine. *J. Physiol. (London)* **268:** 271–289 (1977).
13. Neher, E., and J. H. Steinbach. Local anesthetics transiently block currents through single acetylcholine-receptor channels. *J. Physiol. (London)* **277:** 153–176 (1978).
14. Adler, M., E. X. Albuquerque and F. J. Lebeda. Kinetic analysis of end plate currents altered by atropine and scopolamine. *Mol. Pharmacol.* **14:** 514–529 (1978).
15. Adams, P. R., and B. Sakmann. Decamethonium both opens and blocks endplate channels. *Proc. Nat. Acad. Sci. USA* **75:** 2994–2998 (1978).
16. Colquhoun, D., F. Dreyer and R. E. Sheridan. The actions of tubocurarine at the frog neuromuscular junction. *J. Physiol. (London)* **293:** 247–284 (1979).
17. Albuquerque, E. X., M. Adler, C. E. Spivak and L. Aguayo. Mechanisms of nicotinic channel activation and blockade. *Ann. N.Y. Acad. Sci.* (in press).
18. Gage, P. W., and R. S. Eisenberg. Action potentials without contraction in frog skeletal muscle fibers with disrupted transverse tubules. *Science* **158:** 1702–1703 (1967).
19. Albuquerque, E. X., P. W. Gage and A. C. Oliveira. Differential effect of perhydrohistionicotoxin on 'intrinsic' and 'extrinsic' end-plate responses. *J. Physiol. (London)* **297:** 423–442 (1979).
20. Lapa, A. J., E. X. Albuquerque, J. M. Sarvey, J. Daly and B. Witkop. Effects of histrionicotoxin on the chemosensitive and electrical properties of skeletal muscle. *Exp. Neurol.* **47:** 558–580 (1975).
21. Thesleff, S. The mode of neuromuscular block caused by acetylcholine, nicotine, decamethonium and succinylcholine. *Acta Physiol. Scand.* **34:** 218–231 (1955).
22. Nastuk, W. L. Mechanisms of neuromuscular blockade. *Ann. N.Y. Acad. Sci.* **183:** 171–182 (1971).
23. Wang, C. M., and T. Narahashi. Mechanisms of dual action of nicotine on end-plate membranes. *J. Pharmacol. Exp. Ther.* **182:** 427–441 (1972).
24. Gissen, A. J., and W. L. Nastuk. Succinylcholine and decamethonium: Comparison of depolarization and desensitization. *Anesthesiology* **33:** 611–618 (1970).
25. Dixon, W. J., and M. B. Brown (eds.). *BMDP-79 Biomedical Computer Programs P Series.* University of California Press, Los Angeles, 464–483 (1979).
26. Dionne, V. E., J. H. Steinbach and C. F. Stevens. An analysis of the dose-response relationship at voltage-clamped frog neuromuscular junctions. *J. Physiol. (London)* **281:** 421–444 (1978).
27. Duncan, C. J., and S. J. Publicover. Inhibitory effects of cholinergic agents on the release of transmitter at the frog neuromuscular junction. *J. Physiol. (London)* **294:** 91–103 (1979).
28. Aronstam, R. Cholinergic actions of anatoxin-a. *The Pharmacologist.* **22:** 300, abs. (1980).
29. Ochs, S., and A. K. Mukherjee. Action of acetylcholine, choline and d-tubocurarine on the membrane of frog sartorius muscle fibers. *Amer. J. Physiol.* **196:** 1191–1196 (1959).
30. Varga, E., L. Kovacs and I. Gesztelyi. Analysis of the depolarizing effect of nicotine on frog's skeletal muscle. *Acta Physiol. Acad. Sci. Hung.* **38:** 325–342 (1970).
31. Johnson, E. W., and R. L. Parsons. Characteristics of postjunctional carbamylcholine receptor activation and inhibition. *Amer. J. Physiol.* **222:** 793–799 (1972).
32. Jenkinson, D. H., and D. A. Terrar. Influence of chloride ions on changes in

membrane potential during prolonged application of carbachol to frog skeletal muscle. *Brit. J. Pharmacol.* **47**: 363–376 (1973).
33. Parsons, R. L. Changes in postjunctional receptors with decamethonium and carbamylcholine. *Amer. J. Physiol.* **217**: 805–811 (1969).
34. Martin, A. R. A further study of the statistical composition of the end-plate potential. *J. Physiol.* (*London*) **130**: 114–122 (1955).
35. Beers, W. H., and E. Reich. Structure and activity of acetylcholine. *Nature* **228**: 917–922 (1970).
36. Nakanishi, K. *Infrared Absorption Spectroscopy*. Holden-Day, San Francisco (1962).

Send reprint requests to: E. X. Albuquerque, Department of Pharmacology and Experimental Therapeutics, University of Maryland School of Medicine, Baltimore, Md. 21201.